

Supporting Information

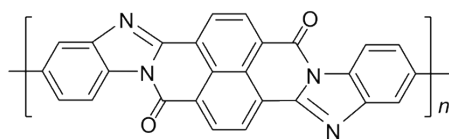
Nanofibre Preparation of Non-processable Polymers by Solid-state Polymerization of Molecularly Self-assembled Monomers

Jian Zhu^{a,b}, Yichun Ding^a, Seema Agarwal^b, Andreas Greiner^{b*}, Hean Zhang^c, and Haoqing Hou^{a*}

^a Department of Chemistry and Chemical Engineering, Jiangxi Normal University, Nanchang, 330022, China. E-mail: haoqing@jxnu.edu.cn

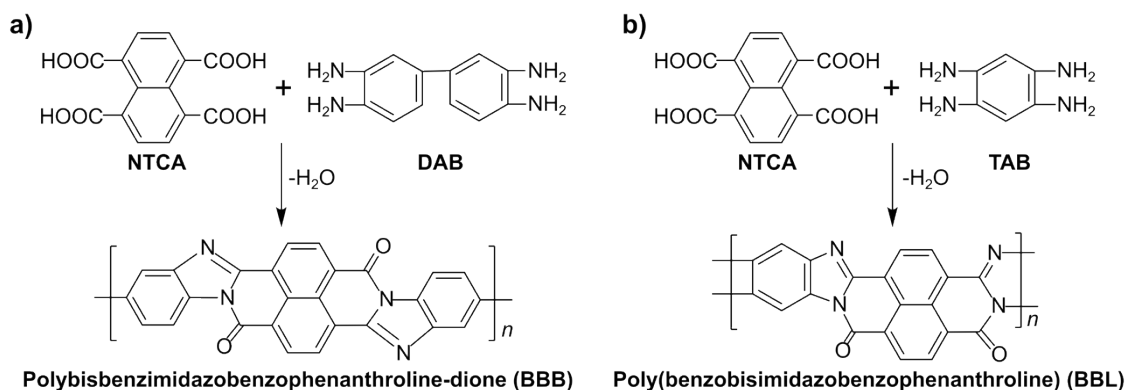
^b Macromolecular Chemistry II and Bayreuth Center for Colloids and Interfaces, University of Bayreuth, Universitätsstrasse 30, 95440, Bayreuth, Germany. E-mail: greiner@uni-bayreuth.de

^c Department of Chemistry, Nanchang University, Nanchang, 330006, China



Polybisbenzimidazobenzophenanthroline-dione (BBB)

Scheme S1. Chemical structure of the BBB polymer.



Scheme S2. Synthesis and chemical structures of (a) BBB and (b) BBL polymers.

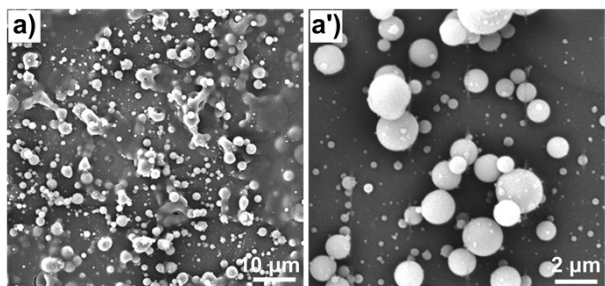


Figure S1. SEM images showing particle formation by the electrospinning of PNDS.

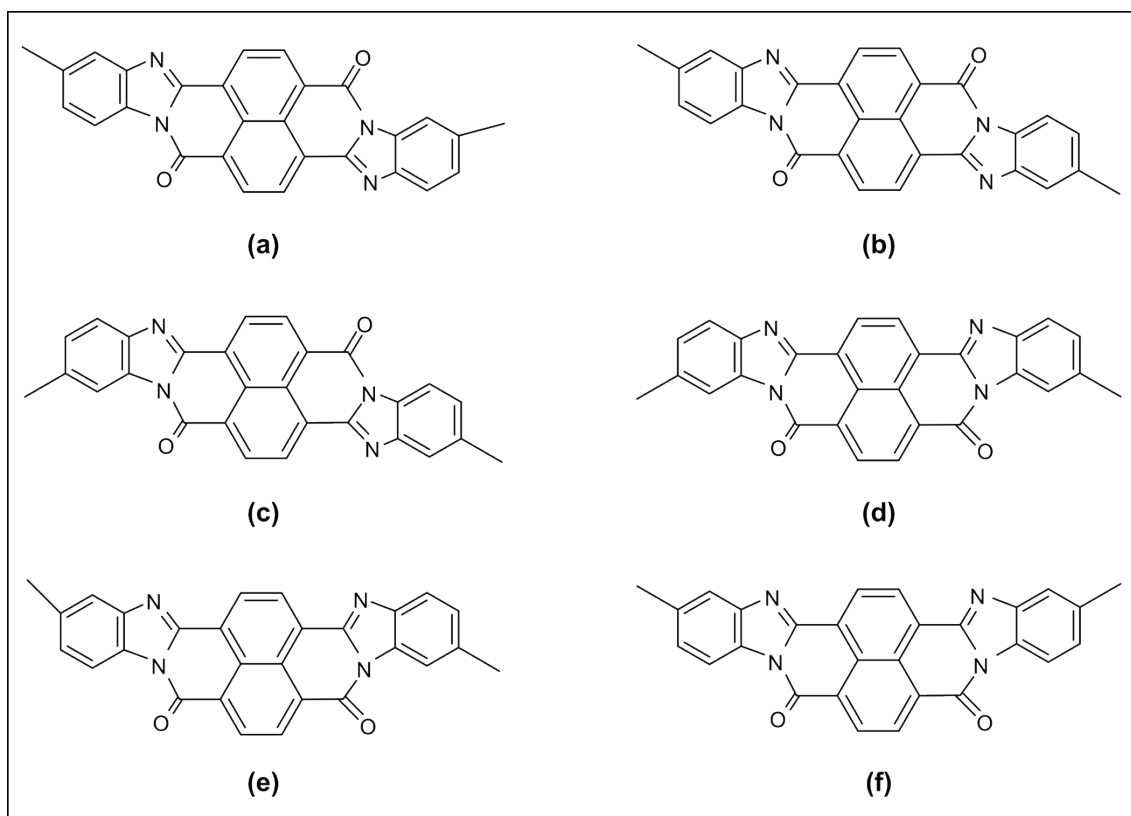


Figure S2. Schematic representation of the repeat unit of BBB isomers¹.

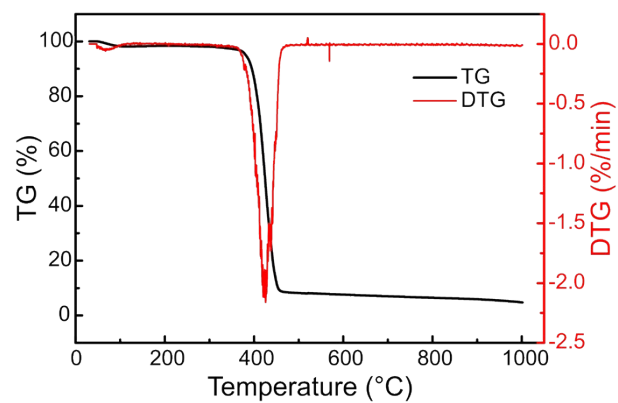


Figure S3. Thermogravimetric analysis (TGA) and DTG curves show the decomposition of neat PVP nanofibres.

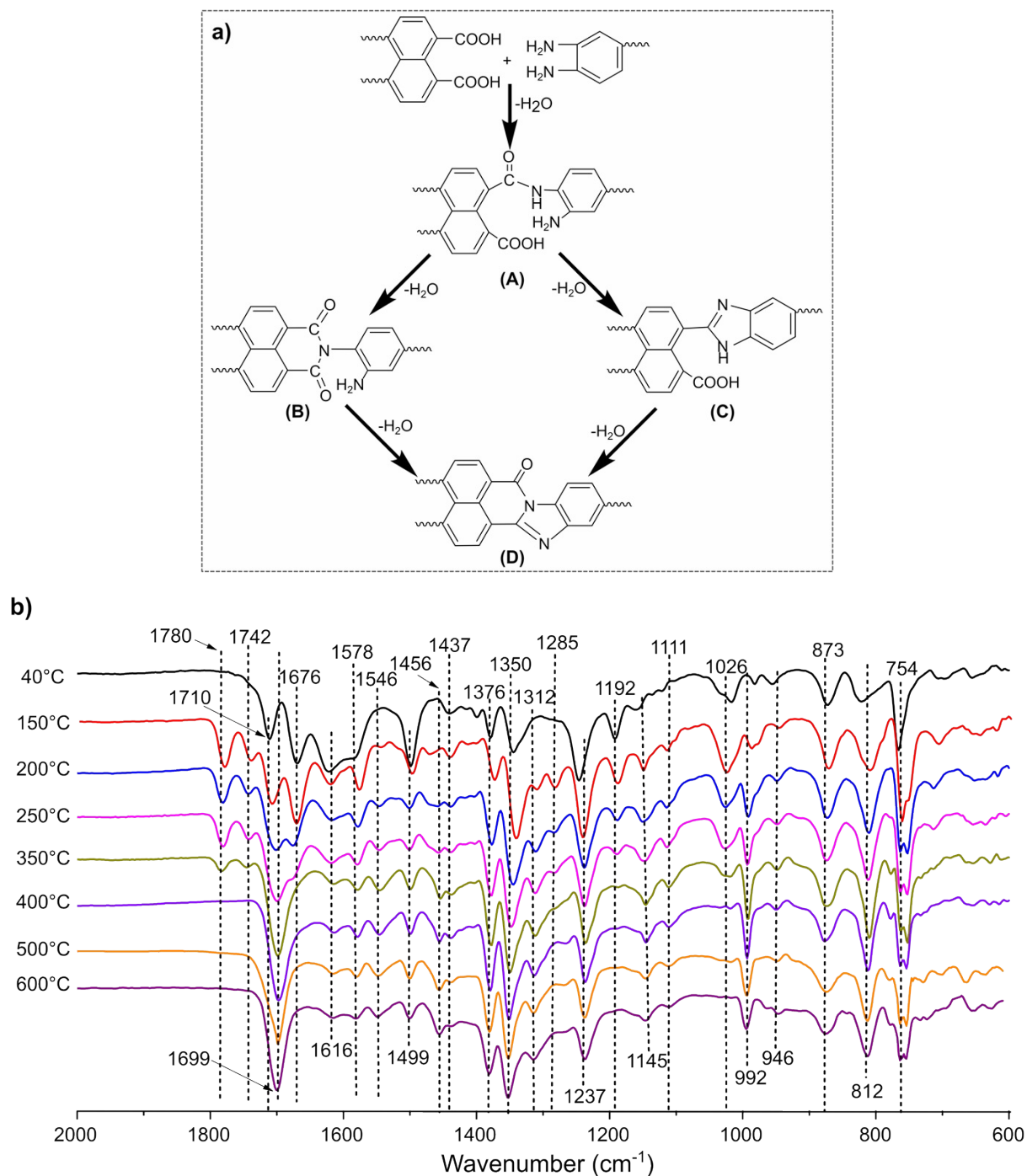
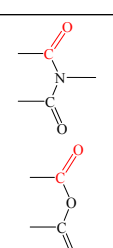
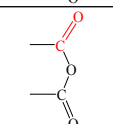
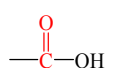
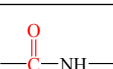
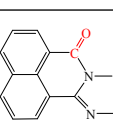
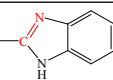
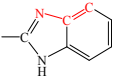
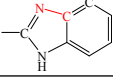
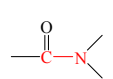
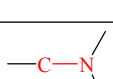
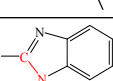
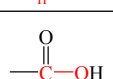
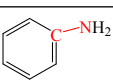
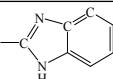
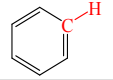
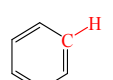
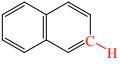


Figure S4. Investigation of BBB polymer formation: a) possible routes for the polymerization of 1,4,5,8-naphthalene tetracarboxylic acid (NTCA) and 3,3'-diaminobenzidine (DAB) to BBB, where possible intermediates include amide (**A**), imide (**B**) and benzimidazole (**C**) structures. b) FTIR spectra of the products formed by heating a 1:1 comonomer mixture of NTCA and DAB at different temperatures.

Table S1. Compilation of results from FT-IR (Figure S4b) regarding the presence of different peaks, signifying different chemical structures at various temperatures.

Absorption	Assignment	40°C	150°C	200°C	250°C	350°C	400°C	500°C	600°C
1780 cm ⁻¹	 $\nu_{(C=O)}$ imide carbonyl carbon-oxygen asymmetric stretching ² ; or $\nu_{(C=O)}$ anhydride carbonyl carbon-oxygen asymmetric stretching ^{3,4}	✓	✓	✓	✓	✓	✗	✗	✗
1742 cm ⁻¹	 $\nu_{(C=O)}$ anhydride carbonyl carbon-oxygen symmetric stretching ³	✗	✓	✓	✓	✓	✗	✗	✗
1710 cm ⁻¹	 $\nu_{(C=O)}$ in carboxyl group	✓ ₁₇₁₀	✓ ₁₇₀₅	✗	✗	✗	✗	✗	✗
1676 cm ⁻¹	 $\nu_{(C=O)}$, in amide carbonyl	✓	✓	✓	✓	✗	✗	✗	✗
1699 cm ⁻¹	 $\nu_{(C=O)}$, imide carbonyl carbon-oxygen stretching in BBB structure ⁵	✗	✗	✓	✓	✓	✓	✓	✓
1578 cm ⁻¹	 $\nu_{(C=N)}$, imine C=N stretching ⁵	✗	✓	✓	✓	✓	✓	✓	✓
1616 cm ⁻¹ 1499 cm ⁻¹	 aromatic C-C and C-N skeletal modes ⁵	✓ ₁₆₂₂ ✓	✓ ₁₆₂₂ ✓	✓ ₁₆₁₉ ✓	✓ ₁₆₁₉ ✓	✓ ₁₆₁₆ ✓	✓ ₁₆₁₆ ✓	✓ ₁₆₁₆ ✓	✓ ₁₆₁₆ ✓
1546 cm ⁻¹ 1312 cm ⁻¹	 C-N skeletal vibrations ⁵	✗ ✗	✓ ✓						
1456 cm ⁻¹ 1437 cm ⁻¹	 $\nu_{(C-N)}$, amide C-N stretching ⁵	✓ ₁₄₄ 2	✓ ₁₄₄ 3	✓ ✓	✓ ✓	✓ ✓	✓ ✓	✓ ✓	✓ ✓
1376 cm ⁻¹ 1350 cm ⁻¹	 $\nu_{(C-N)}$ of carbon-nitrogen single bonds ⁵	✓ ✓ ₁₃₄₄	✓ ✓ ₁₃₄₄	✓ ✓ ₁₃₄₄	✓ ✓ ₁₃₄₈	✓ ✓ ₁₃₅₀	✓ ✓ ₁₃₅₁	✓ ✓ ₁₃₅₂	✓ ✓ ₁₃₅₂
1285 cm ⁻¹	 breathing vibration of the imidazole ring (C-N-H) ⁶	✓	✓	✓	✓	✗	✗	✗	✗
1192 cm ⁻¹	 $\nu_{(C-O)}$ in carboxyl group	✓	✓	✓	✓	✗	✗	✗	✗
1026 cm ⁻¹	 $\nu_{(C-N)}$, C-N stretching of C-NH ₂	✓	✓	✓	✓	✓	✗	✗	✗
1237 cm ⁻¹ 992 cm ⁻¹	 aromatic skeletal vibrations ⁵	✓ ₁₂₄₇ ✗	✓ ₁₂₄₃ ✓	✓ ₁₂₃₈ ✓	✓ ₁₂₃₇ ✓	✗ ₁₂₃₆ ✓	✗ ₁₂₃₆ ✓	✗ ₁₂₃₆ ✓	✗ ₁₂₃₆ ✓
1145 cm ⁻¹ 1111 cm ⁻¹	 in-plane C-H bending ⁵	✓ ₁₁₅₈ ✓ ₁₁₁₆	✓ ₁₁₅₂ ✓ ₁₁₁₆	✓ ₁₁₅₀ ✓ ₁₁₁₃	✓ ₁₁₄₇ ✓ ₁₁₁₁	✓ ₁₁₄₆ ✓ ₁₁₁₁	✓ ₁₁₄₅ ✓ ₁₁₁₁	✓ ₁₁₄₅ ✓ ₁₁₁₁	✓ ₁₁₄₅ ✓ ₁₁₁₁
946 cm ⁻¹ 873 cm ⁻¹ 812 cm ⁻¹	 out-of-plane C-H wagging ⁵	✓ ✓ ✓							

754 cm ⁻¹		(C-H), out-of-plane wag of naphthalene C-H bonds 5	✓	✓	✓	✓	✓	✓	✓	✓
----------------------	---	--	---	---	---	---	---	---	---	---

*Note: The tick mark indicates absorption, and the x mark indicates no absorption; a small mark indicates low absorption, and large mark indicates high absorption. A mark with a subscript indicates that the absorption has a peak shift.

Investigation of BBB polymer formation: Due to the multi-functionality of NTCA and DAB, the formation of the BBB polymer is a complicated process. The polycondensation between amino and acid groups can occur via several different routes. Typically, it can form an amide structure (structure **A**, **Figure S4a**) by losing one H₂O molecule in each repeat unit and can form an imide structure (structure **B**, **Figure S4a**) or a benzimidazole structure (structure **C**, **Figure S4a**) by losing two H₂O molecules in each repeat unit^{4, 7}. The imide and benzimidazole structures could convert to BBB (structure **D**, **Figure S4a**) by losing an additional H₂O molecule in each repeat unit. To further understand the thermally induced formation of the BBB polymer, we investigated the polycondensation reaction by FTIR. The two monomers were dissolved in dimethylacetamide in equimolar ratios and precipitated in ethanol, and the powder was heated at different temperatures (40, 150, 200, 250, 350, 400, 500, or 600°C) for 1 h at each temperature. The FT-IR spectra of the samples are shown in **Figure S4b**, and the characteristic absorptions are listed in **Table S1**.

At 40°C, the characteristic absorptions of -COOH ($\nu_{(C=O)}$ at 1710 cm⁻¹, $\nu_{(C-O)}$ at 1192 cm⁻¹) and -C-NH₂ (deformation vibration of -NH₂ at 1026 cm⁻¹) were seen. Absorptions at 1676 and 1437 cm⁻¹ corresponding to the $\nu_{(C=O)}$ and the C-N stretching in amides (-C(O)-NH-) were also observed, indicating the formation of an amide structure (structure **B**, **Figure S4a**). The peaks at 1616 and 1499 cm⁻¹ correspond to C=C in the aromatic benzene skeleton, 1376 and 1350 cm⁻¹ correspond to carbon-nitrogen single bonds, and 1237, 946, 873, 812 and 754 cm⁻¹

correspond to aromatic skeleton vibrations and in-plane and out-of-plane C-H bending modes. When heat treated at 150°C, new absorptions at 1780 cm⁻¹ and 1705 cm⁻¹ (an overlap peak with C=O in -COOH) were observed, which are likely to be due to the asymmetric and symmetric vibrations of C=O in the carbonyl imide ring⁸ indicating the formation of an imide structure (molecule **B**, **Figure S4a**). In addition, new absorptions at 1578 and 1285 cm⁻¹ were also observed, these peaks correspond to C=N and C-N-H in the imidazole ring, respectively⁶, indicating the formation of a benzimidazole structure (molecule **C**, **Figure S4a**). In addition, the formation of end dianhydride groups is indicated by characteristic peaks at 1780 cm⁻¹ (asymmetric vibrations of C=O) and 1742 cm⁻¹ (symmetric vibrations of C=O)³. Hence, the reaction of NTCA and DAB began at 150°C, in which the intermediate is a mixture of amide, imide and benzimidazole structures. With a further increase in the temperature to 200°C, the absorptions at 1710 and 1676 cm⁻¹ began to disappear, and a new signal appeared at 1699 cm⁻¹ ($\nu_{\text{C=O}}$ in the BBB structure), indicating the formation of the BBB structure. The absorptions at 1710 and 1676 cm⁻¹ almost completely disappeared, and the intensity of the absorption at 1699 cm⁻¹ became strong at temperatures above 250°C. In addition, the characteristic peak of benzimidazole at 1285 cm⁻¹ almost completely disappeared at 250°C. These phenomena demonstrate the conversion of amide, imide and benzimidazole structures into the BBB polymer. In addition, the characteristic peaks of end dianhydride groups at 1780 and 1742 cm⁻¹ continuously weakened with an increase in temperature and finally disappeared at above 400°C (400, 500, and 600°C), indicating an increase in molecular weight with an increase in heat-treatment temperature. Finally, at 350, 400, 500, and 600°C, the absorptions at 1699, 1616, 1578 and 1547 cm⁻¹, corresponding to the C=O, C=C, C=N and C-N, respectively, on aromatic imide and benzimidazole structures, confirm the formation of the BBB polymer.

Hence, neat BBB nanofibres could be obtained by the heat treatment of PNDS/PVP above 460°C (see experimental details described in the main text) because the NTCA and DAB could be completely converted into BBB at temperatures above 250°C and PVP could be completely decomposed at temperatures above 460°C.

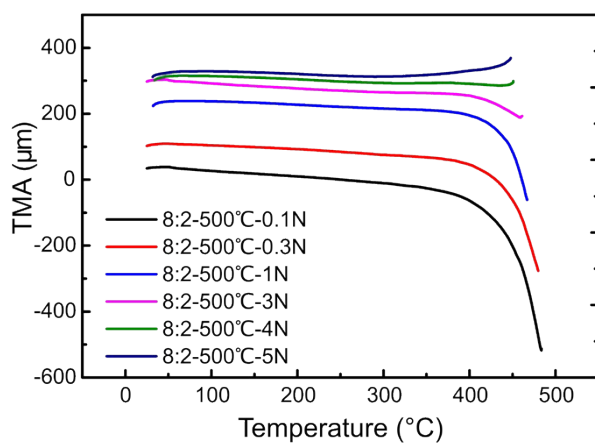


Figure S5. Thermal-shrinkage behaviour of BBB nanofibre belts: BBB nanofibre belts (prepared from PNDS/PVP (8:2); heating at 500°C) with an initial length of 10 mm and a width of 4 mm were fixed on the DMA instrument, and different constant tension forces (*i.e.*, 0.1, 0.3, 1, 3, 4 and 5 N) were applied. The results showed that the shrinkage at 450°C was only 1.16% under 5 N tension force and 4.8% under 0.1 N.

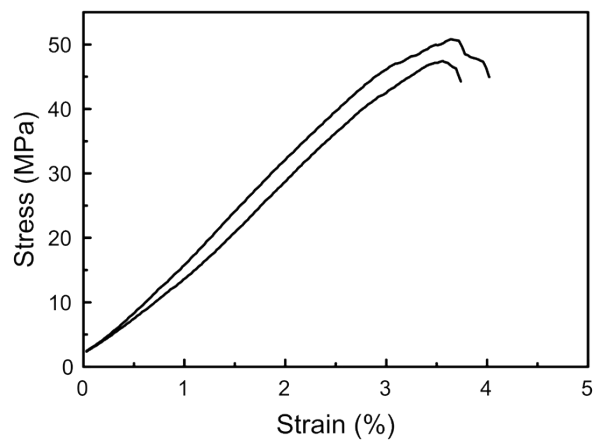


Figure S6. Stress-strain curves of the PNDS/PVP (8:2) composite nanofibre belt.

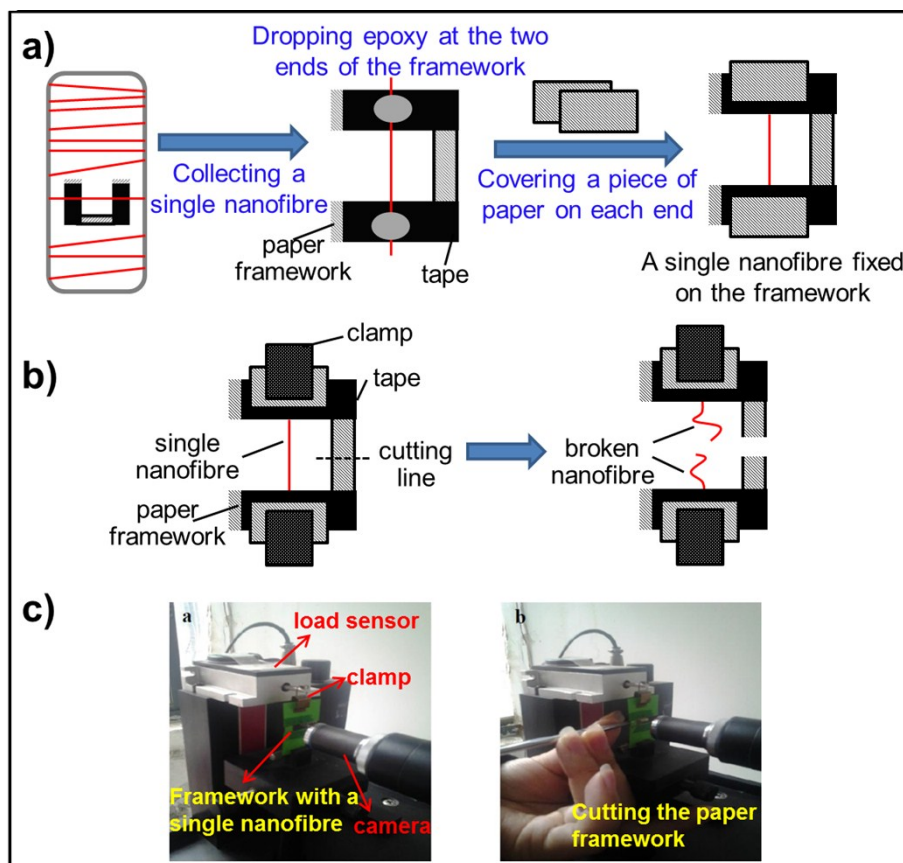


Figure S7. Mechanical characterization of a single BBB nanofibre: a) schematic of picking a single BBB nanofibre and fixing on a paper framework, b) schematic diagram of the paper framework holding a single nanofibre in the clamps for the tension test and cutting the paper frame to perform the tensile test, and c) optical image of the single nanofibre testing machine holding the sample and the process of cutting the paper framework.

Mechanical characterization of a single BBB nanofibre: Tensile tests of single electrospun nanofibres were performed on a microtensile testing machine (JQ03, Power-Reach Digital Equipment Ltd., Shanghai, China). The tensile tester consisted of a 19.6 mN to 0.50 μ N microload sensor (Minebea Co., Ltd, Japan), a high-magnification optical microscope (MS160, WDK, Japan), a digital camera, software for data acquisition and processing and a computerized control system. The test method was the same as that previously reported by

us⁹⁻¹¹. The testing process consists of five steps: 1) load the single nanofibre sample onto the paper framework (**Figure S7a**), 2) mount the paper framework carrying the single nanofibre sample in the clamps of the microtensile tester, 3) cut the ‘rib’ of the paper frame (**Figure S7c**), 4) locate the nanofibre sample using the optical microscope to ensure that only one nanofibre sample is present, and 5) load the single nanofibre sample to break with the microtension tester (**Figure S7c**). A constant loading rate of 1 mm/min was utilized over the entire tensile testing process.

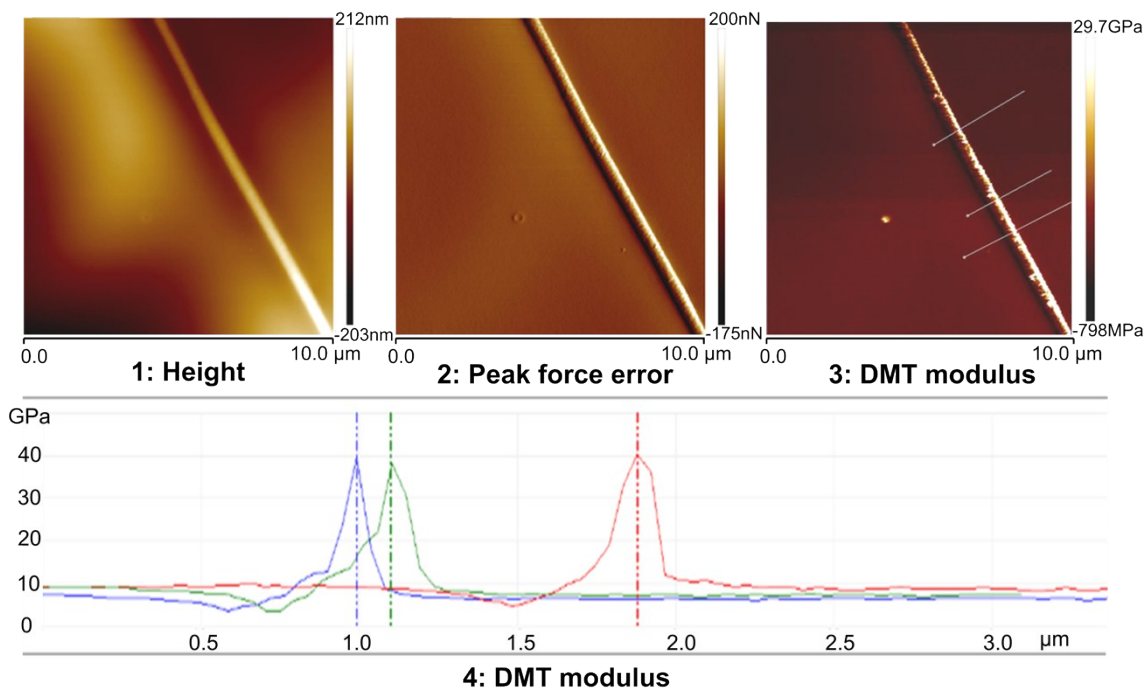


Figure S8. Nanomechanical characterization of BBB single nanofibres using scanning probe microscopy (SPM) and peak force (PF) quantitative nanoscale mechanical (QNM) characterization: maps of the typical height, peak force error and DMT modulus (Derjaguin-Muller-Toropov model) of BBB individual nanofibres.

Table S2 Summary of mechanical properties of different types of BBB nanofibre belts.

BBB belts*	Stress (MPa)	Strain at break (%)	Modulus (GPa)
8:2-460°C	242.57±10.72	33.49±2.61	2.70±0.48
8:2-480°C	291.73±13.23	23.15±1.48	2.73±0.12
8:2-500°C	364.75±4.76	23.66±3.01	2.73±0.2
8:2-520°C	323.15±16.84	17.95±1.03	3.08±0.26
8:2-540°C	312.26±27.48	16.13±1.67	3.3±0.12
8:2-580°C	263.42±16.89	8.84±1.12	4.12±0.69
6:4-500°C	378.05±3.55	20.1±0.53	3.19±0.18
7:3-500°C	339.45±14.13	19.91±2.32	3.24±0.35

*Sample designation: m:n-y°C, m:n is the weight ratio of NTCA+DAB: PVP, y is the temperature used for heating the PND/S/PVP composite fibres to convert them to BBB nanofibres.

References

1. G. C. Berry and T. G. Fox, *Journal of Macromolecular Science: Part A - Chemistry*, 1969, **3**, 1125-1146.
2. C. A. Pryde, *Journal of Polymer Science Part A: Polymer Chemistry*, 1989, **27**, 711-724.
3. N. Srinate, S. Thongyai, R. A. Weiss and P. Prasertdam, *J Polym Res*, 2013, **20**, 138.
4. V. G. Ammons and G. C. Berry, *Journal of Polymer Science Part A-2: Polymer Physics*, 1972, **10**, 449-471.
5. M. F. Roberts and S. A. Jenekhe, *Polymer*, 1994, **35**, 4313-4325.
6. H. Luo, H. Pu, Z. Chang, D. Wan and H. Pan, *Journal of Materials Chemistry*, 2012, **22**, 20696-20705.
7. R. L. Van Deusen, O. K. Goins and A. J. Sicree, *Journal of Polymer Science Part A-1: Polymer Chemistry*, 1968, **6**, 1777-1793.
8. A. Li, Z. Ma, H. Song, N. Li and M. Hou, *RSC Advances*, 2015, **5**, 79565-79571.
9. F. Chen, X. Peng, T. Li, S. Chen, X.-F. Wu, D. Reneker, H. and H. Hou, *Journal of Physics D: Applied Physics*, 2008, **41**, 025308.
10. S. Jiang, G. Duan, E. Zussman, A. Greiner and S. Agarwal, *ACS Applied Materials & Interfaces*, 2014, **6**, 5918-5923.
11. L. Chen, S. Jiang, J. Chen, F. Chen, Y. He, Y. Zhu and H. Hou, *New Journal of Chemistry*, 2015, **39**, 8956-8963.